A *Classical* Kinetic Theory Approach to Lattice Boltzmann Simulation

by

Nicos S. Martys
Building and Fire Research Laboratory
National Institute of Standards and Technology
Gaithersburg, MD 20899 USA

Reprinted from International Journal of Modern Physics C, Vol. 12, No. 8, 1169-1178, October 2001.

NIST
National Institute of Standards and Technology
Technology Administration, U.S. Department of Commerce

International Journal of Modern Physics C, Vol. 12, No. 8 (2001) 1169–1178

A *CLASSICAL* KINETIC THEORY APPROACH TO LATTICE BOLTZMANN SIMULATION

NICOS S. MARTYS

Building Materials Division, Building and Fire Research Laboratory
National Institute of Standards and Technology
Gaithersburg, Maryland 20899, USA

Received 20 July 2001
Revised 20 July 2001

An approach to lattice Boltzmann simulation is described, which makes a direct connection between classical kinetic theory and contemporary lattice Boltzmann modeling methods. This approach can lead to greater accuracy, improved numerical stability and significant reductions in computational needs, while giving a new philosophical point of view to lattice Boltzmann calculations for a large range of applications.

Keywords: BGK; Complex Fluids; Computational Fluid Dynamics; Kinetic Theory; Lattice Boltzmann; Navier–Stokes Equation; Phase Transitions; Porous Media.

The flow of complex fluids or fluid flow in complex geometries plays an important role in a wide variety of technological and environmental processes such as in the manufacturing and utilization of polymer blends,[1] the spread of hazardous wastes in soils[2] and oil recovery.[2,3] The study of complex fluids is also of fundamental interest and has been the subject of intense research in recent years. Problems of fundamental interest include the characterization of critical properties of phase separating binary mixtures,[4] the formation of a string morphology in polymer blends under shear,[5] contact line motion over a heterogeneous surface,[6] and the role of disorder in multiphase flow in porous media.[2,3,7] While the numerical simulation of complex fluid systems remains a great challenge, there have been many advances in cellular automata-based methods for describing such complex flows over the last 15 years. Early approaches include lattice-gas automata,[8,9] where a given number of particles are allowed to move and collide under a set of rules that are designed such that the time-averaged motion of the particles is consistent with the Navier–Stokes equation. An outgrowth of the lattice-gas based models was the lattice Boltzmann method,[10] where, instead of tracking each particle, the time evolution of the single-particle velocity distribution function was determined. Later, lattice Boltzmann models[11,12] were formulated to remove certain unphysical features found in both lattice-gas and earlier lattice Boltzmann models, including the lack of Galilean invariance and the

velocity dependence of the pressure field.[11,12] Newer versions of such algorithms can model phase transitions and multicomponent fluid systems.[9,13–15]

Central to all of the above described methods is the proper construction of the collision operator. For example, lattice-gas models depend on the construction of collision tables, while most lattice Boltzmann (LB) based models use the BGK collision operator[11,12] due to its simplicity and ability to recover the Navier–Stokes equation in certain limits. A serious problem with the lattice Boltzmann BGK model is that it often does not satisfactorily account for many boundary conditions, especially when the viscosity of the fluid is large, and can be unstable when there is a large density or viscosity mismatch in the fluid system.[16] More importantly, there is still considerable debate over the correct physical basis and formulation of the collision operator when modeling a nonideal gas or a multicomponent fluid.[9,13–15] In many cases, the LB method can be thought of as a "top down" approach, where computational algorithms are constructed to model certain macroscopic phenomena without necessarily being true to the underlying microscopic physics. As kinetic theory is considered fundamental, it is crucial to make a strong connection between kinetic theory and lattice Boltzmann computational methods. Until recently, a considerable body of research concerning *classical* kinetic theory[17–19] was seldom used as a basis to develop LB theory. However, over the past few years, there has been significant progress in making a connection between the continuum BGK equation and lattice Boltzmann BGK methods.[20] Also, a clear connection between BBGKY theory and construction of a mean-field-theory LB model of multicomponent fluid systems has been established.[21]

In this paper, I examine an approach to solve for the time evolution of the single-particle distribution function described by any of the usual kinetic equations[17]: BGK and Boltzmann equations, and other related versions such as the Enskog hard sphere model, to any order of its associated Chapman–Enskog expansion.[17,18] For example, because physical information is retained with respect to the order of the Chapman–Enskog expansion, this approach naturally recovers the Euler equations and Navier–Stokes equations.

The key idea is, once the form of the distribution function is known to a particular order, one can reformulate the collision operator to reflect this information. This method can be implemented in traditional BGK based LB models, significantly improving their accuracy with the added bonus of large reductions on computational memory requirements by restriction of the single particle velocity distribution function to the first order of Chapman–Enskog expansion. In addition, this approach allows for the application of many computational fluid dynamics methods that can significantly improve the accuracy of the solution over that of more traditional lattice Boltzmann methods, including improved modeling of flow near solid boundaries and at a fluid/fluid interface. Finally, and perhaps most important, the lattice Boltzmann method now becomes an ideal "mesoscopic" approach, which makes a direct connection between microscopic and macroscopic phenomena.

First consider the continuum Boltzmann equation

$$\partial_t f + \mathbf{v} \cdot \nabla f + \mathbf{a} \cdot \nabla_v f = \Omega \,, \tag{1}$$

where f is the single-particle velocity distribution function, $\mathbf{v}$ is the microscopic velocity, Ω is the collision operator and $\mathbf{a} = \mathbf{F}/\rho$ is the acceleration due to a body force $\mathbf{F}$. The macroscopic variables density, velocity, and temperature, denoted by ρ, $\mathbf{u}$, and T, respectively, are obtained from the following moments of the single-particle distribution function: $\rho = m \int f d^3v$, $\rho \mathbf{u} = m \int \mathbf{v} f d^3v$, and $T = (m/3k_b) \int (\mathbf{u} - \mathbf{v})^2 f d^3v$, where m is the mass and k_b is the Boltzmann constant.

In order to determine the time evolution of the above macroscopic variables as well as to relate other macroscopic fluid properties, such as viscosity and thermal conductivity, to the microscopic properties of the system, Chapman and Enskog independently developed a procedure to create a hierarchy of approximate solutions to the Boltzmann equation. They were then able to separate the physical phenomena associated with different time and length scales. The main idea of the Chapman–Enskog procedure[17,18] is to write the single-particle velocity distribution as $f = f^{(0)} + f^{(1)} + f^{(2)} \cdots$, where, $f^{(1)} = f^{(0)} \phi^{(1)}$, $f^{(2)} = f^{(0)} \phi^{(2)}$. Here, $f^{(0)}$ is the equilibrium distribution function

$$f^{(0)} = \frac{n}{(2\pi m k_b T)^{3/2}} \exp\left(\frac{-mU^2}{2k_b T}\right), \tag{2}$$

with number density, n, and $\mathbf{U} = \mathbf{v} - \mathbf{u}$. The function ϕ contains information about spatial gradients in the fluid system. To isolate phenomena important at different time scales, the time derivative is also expanded as follows:

$$\frac{\partial}{\partial t} = \frac{\partial}{\partial t_0} + \frac{\partial}{\partial t_1} + \cdots \,, \tag{3}$$

where the lowest-order terms vary most rapidly. One may now construct a PDE associated with each order of the Chapman–Enskog expansion. To the zeroth order, one obtains:

$$\frac{\partial f}{\partial t} = \frac{\partial f^{(0)}}{\partial t_0} = \frac{\partial f^{(0)}}{\partial \rho} \frac{\partial \rho}{\partial t_0} + \frac{\partial f^{(0)}}{\partial u_i} \frac{\partial u_i}{\partial t_0} + \frac{\partial f^{(0)}}{\partial T} \frac{\partial T}{\partial t_0} \,. \tag{4}$$

The time derivatives of the macroscopic variables are obtained from the Chapman–Enskog analysis[17,18] and are:

$$\frac{\partial \rho}{\partial t_0} = -\nabla \cdot \rho \mathbf{u} \,,$$

$$\rho \frac{\partial \mathbf{u}}{\partial t_0} = -\rho (\mathbf{u} \cdot \nabla) \mathbf{u} - \nabla \cdot \overleftrightarrow{P}^0 \,,$$

$$\rho \frac{\partial T}{\partial t_0} = -\rho (\mathbf{u} \cdot \nabla) T - \frac{2}{3} \frac{m}{k_b} \overleftrightarrow{P}^0 : \overleftrightarrow{\Lambda} \,,$$

where

$$\Lambda_{ij} = \frac{1}{2}\left(\frac{\partial v_i}{\partial x_j} + \frac{\partial v_j}{\partial x_i}\right)$$

and the pressures tensor $P^0_{ij} = nk_bT\delta_{ij}$. Clearly, this zeroth order form is consistent with the Euler equations.

Next note, to first order, the single particle distribution evolves in time according to:

$$\frac{\partial f}{\partial t} = \frac{\partial f}{\partial t_0} + \frac{\partial f}{\partial t_1} = \frac{\partial (f^{(0)} + f^{(1)})}{\partial t_0} + \frac{\partial f^{(0)}}{\partial t_1}$$
$$= \frac{\partial f^{(0)}}{\partial t_0}(1 + \phi^{(1)}) + \frac{\partial f^{(0)}}{\partial t_1} + f^{(0)}\frac{\partial \phi^{(1)}}{\partial t_0}. \tag{5}$$

The t_1 derivatives of the macroscopic variables, obtained from the Chapman–Enskog analysis,[17,18] are:

$$\frac{\partial \rho}{\partial t_1} = 0,$$

$$\rho\frac{\partial \mathbf{u}}{\partial t_1} = -\nabla \cdot \overleftrightarrow{P^1},$$

$$\rho\frac{\partial T}{\partial t_1} = -\frac{2}{3}\frac{m}{k_b}(\overleftrightarrow{P^{(1)}} : \overleftrightarrow{\Lambda} + \nabla \mathbf{Q}^{(1)})$$

with

$$P^{(1)}_{ij} = \int f^{(1)} U_i U_j d\mathbf{U} \quad \text{and} \quad Q^{(1)}_i = \int f^{(1)}\frac{m}{2} U^2 U_i d\mathbf{U}.$$

To complete the first order equation, $\phi^{(1)}$, which depends on the collision operator, is needed. For example, consider the BGK Boltzmann equation, where the collision operator is represented by $\Omega = (1/\tau)(f^{(0)} - f)$ so that, to the first order in the Chapman–Enskog expansion,

$$\Omega \approx \frac{1}{\tau} f^{(1)} = \frac{1}{\tau} f^{(0)}\phi^{(1)}.$$

Inserting $f^{(0)}$ into the left hand side of Eq. (1), it is found that

$$f^1 = f^{(0)}\phi^{(1)} = -f^{(0)}\frac{\tau}{k_bT}\left[\left(\frac{m}{2k_bT}U^2 - \frac{5}{2}\right)(\mathbf{U}\cdot\nabla k_bT)\right.$$
$$\left. + m\sum_{i,j=1}^{3}\Lambda_{i,j}\left(U_iU_j - \frac{1}{3}\delta_{ij}U^2\right)\right]. \tag{6}$$

At the first order approximation, the time evolution of f is consistent with the continuity, Navier–Stokes, and heat equation with viscosity and thermal conductivity proportional to τ. The derivation of $\phi^{(1)}$ for other collision operators may be found in the literature.[17,18]

With the expansion procedure layed out, the next question is how can such information be incorporated into a numerical algorithm to solve for the time evolution of the single particle distribution function. Several possible approaches are given below. For example, once the PDE for the single-particle distribution function is determined to the order needed [i.e., Eqs. (4) or (5)], where all quantities are represented in terms of the macroscopic variables of density, velocity, temperature and the microscopic velocity, the PDE may be discretized in a velocity phase space[20] associated with the microscopic velocities. Therefore, $f \rightarrow f_i$, $f^0 \rightarrow f_i^0$, and $\mathbf{U} = \boldsymbol{\nu} - \mathbf{u} \rightarrow \boldsymbol{\nu}_i - \mathbf{u}$, where the index i corresponds to the discretized microscopic velocity. In addition, the equilibrium distribution can be replaced by its representation as a truncated Hermite polynomial in discrete velocity space, as is typical in lattice Boltzmann simulations.[15,20] Because the microscopic velocities form a discrete set, the integrals that define the macroscopic variables (or their respective time derivatives) are now replaced by sums. Equations for the single-particle distribution function can then be numerically integrated by a variety of computational schemes.

For illustrative purposes, the case of pressure-driven flow between parallel plates is studied. While this is an extremely simple flow geometry, it also serves to illustrate a serious flaw with the physical interpretation of the usual lattice Boltzmann method. We examine the isothermal limit and hence neglect terms with temperature gradients. For this example, a lattice Boltzmann model based on the D3Q19 lattice (three dimensional lattice with 19 microscopic velocities) will be utilized.[12] Results can be easily generalized to other lattice models. The microscopic velocities, $\mathbf{v}_i$, equal all permutations of $(\pm 1, \pm 1, 0)$ for $1 \leq i \leq 12$, $(\pm 1, 0, 0)$ for $13 \leq i \leq 18$, and $(0, 0, 0)$ for $i = 19$. The units of $\mathbf{v}_i$ are the lattice constant divided by the time step. Macroscopic quantities such as the density and fluid velocity are obtained by taking suitable moment sums of f_i. Here, $\rho = m \sum_i f_i$ and $\rho \mathbf{u} = m \sum_i f_i \mathbf{v}_i$. In our units, the molecular mass m equals 1. The equilibrium distribution takes the following form[11,12]:

$$f_i^{(0)} = t_i \rho \left[1 + 3\mathbf{v}_i \cdot \mathbf{u} + \frac{3}{2} (3\mathbf{v}_i \mathbf{v}_i : \mathbf{u}\mathbf{u} - u^2) \right], \tag{7}$$

with, $t_i = 1/36$ for $1 \leq i \leq 12$, $t_i = 1/18$ for $13 \leq i \leq 18$ and $t_{19} = 1/3$. A second order Runge–Kutta scheme is used to integrate the equations of motion [Eqs. (4) or (5)]. In the zeroth order limit of the Chapman–Enskog expansion, numerical solution of the PDE [Eq. (4)] results in a flat velocity profile between the parallel plates (Fig. 1) because there are no viscous effects here, consistent with solution of the Euler equations. At the next order of the Chapman–Enskog expansion [Eq. (5)], a parabolic velocity profile is obtained as the viscous effects become important. Data are also included for the case where the viscosity is increased by a factor of 40. Note the good overlap as the data are scaled to account for the difference of viscosity. It should be emphasized that this degree of agreement has not been obtained in usual three-dimensional lattice Boltzmann methods (see Fig. 1 for comparison to a standard LB method).[16] This example illustrates that, when modeling a multicomponent fluid with a large viscosity mismatch, the usual lattice Boltzmann method

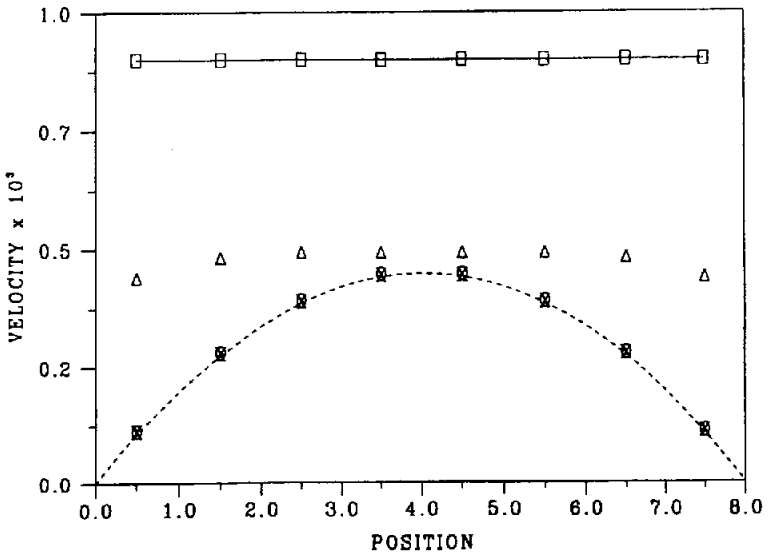

Fig. 1. Velocity field between parallel plates based on numerical simulation data for the case of the zeroth order Chapman–Enskog expansion (squares) and the first order Chapman–Enskog expansion where circles correspond to $\tau = 1$ and the x' correspond to $\tau = 40$. The velocity field for the $\tau = 40$ case is multipled by a factor of 40. The dashed line is the solution of the Navier–Stokes equation for the same boundary conditions. The triangles are from a lattice Boltzmann simulation with $\tau = 40$. For this simulation, a second order accurate bounce-back algorithm was implemented at the walls. Data (triangles) are shifted up slightly to more clearly see the exact solution. Note the large slip velocity near the walls for the lattice Boltzmann case. Velocity units are lattice spacing divided by the lattice Boltzmann time step.

can produce inconsistent results, where each fluid effectively has a different slip velocity depending on its viscosity. Further, a Chapman–Enskog expansion applied to the usual BGK lattice Boltzmann method shows a departure from Navier–Stokes that goes as a power series in τ so that the method becomes hopelessly inaccurate as τ or viscosity is increased.

Although the above example shows that a lattice Boltzmann based simulation can be formulated to obtain a direct mapping to the Navier–Stokes equations, its implementation is rather cumbersome. Further, an important advantage of the more traditional BGK lattice Boltzmann method is its natural formulation as an upwind scheme so that it is not necessary to determine the flow direction to select the form of spatial gradient operator. To circumvent some of the above described limitations of lattice Boltzmann BGK while preserving the up-wind formulation, one may simply make the replacement $f_i \to f_i^{(0)} + f_i^{(1)}$ in the usual lattice Boltzmann model. An important benefit is that once the distribution function is replaced with its Chapman–Enskog expansion, saving each f_i in computer memory is no longer necessary because its first order approximation can be entirely constructed from the macroscopic variables (i.e., typically, 15 to 19 f_i are needed for isothermal models

and 34+ for thermal models) resulting in a significant computational memory reduction for many practical applications. It should be pointed out that, in contrast to the usual lattice Boltzmann method, one must now calculate spatial derivatives of velocity (and temperature in a thermal model). However, this was not found to be an excessive burden when implementing the algorithm. Numerical tests were performed on this algorithm and it was found to agree well with standard lattice Boltzmann for $\tau < 1$. Unfortunately, it was found that this approach became unstable for $\tau \simeq 2$.

An alternate approach is to formulate the algorithm, using the Chapman–Enskog expansion of the single particle distribution function only, as a finite difference code as described in Ref. 16 and choose a small enough time step. As a check, simulations of fluid flow around a periodic array of spheres were carried out and it was found that, in the low Reynolds limits, the permeability, k, (as defined by Darcy's law $\langle \mathbf{u} \rangle = -(k/\mu)\langle \nabla P \rangle$ with viscosity, μ and $\langle \nabla P \rangle$ the average pressure gradient) was independent of τ for $100 < \tau < 1$ and, indeed, consistent with solution of the Stokes equations. In contrast, a numerical determination of permeability using a traditional lattice Boltzmann methods would show a strong dependence on τ because of the slip phenomena indicated in Fig. 1. It should be mentioned that previous studies have shown that improvements to the slip boundary condition can also be obtained using a generalized lattice Boltzmann scheme having multiple relaxation times,[22] however, the method used in this paper is based on a simpler single time relaxation method.

The approach described above in this paper is quite general. The functional form of $\phi^{(1)}$ has been derived for other models including the usual Boltzmann and Enskog hard sphere models and may also be extended to model multicomponent fluid systems as in the work of Lopez de Haro, Cohen and Kincaid.[19] In the same spirit, other non-Chapman–Enskog based representations of the single particle distribution function (i.e., Grad's method of moments[17,18]), which avoid explicit inclusion of velocity gradients, can instead be utilized. For example, consider the D3Q19 lattice model described earlier. In this case, f_i is replaced by f_i^g:

$$f_i^g = f_i^0 + \frac{1}{2} t_i \overleftrightarrow{b}_i : (3\mathbf{v}_i\mathbf{v}_i - \overleftrightarrow{1}), \tag{8}$$

where $\overleftrightarrow{b}_i = \sum_i (3\mathbf{v}_i\mathbf{v}_i - \overleftrightarrow{1}) g_i$ and $g_i(\mathbf{x}, t) = f_i^g(\mathbf{x} - \mathbf{v}_i, t-1) + \Omega(\mathbf{x} - \mathbf{v}_i, t-1)$. Again, there is a saving in computational memory because, for the isothermal case in 3D, f_i^g depends on 10 quantities ρ, $\mathbf{u}$, and $\overleftrightarrow{b}$ (note $\overleftrightarrow{b}$ is symmetric). Indeed, we have found that when adopting Grad's method of moments, good agreement is found with BGK lattice Boltzmann for $\tau < 1$ and that the solution for the flow fields near a solid surface for $\tau > 1$ was improved. The $\tau = 1$ case is identical to lattice Boltzmann.

Finally, the approach described in this paper can be extended to model liquid/gas phase transitions or phase separation of multicomponent fluid systems due to long-range molecular forces. Here, the collision operator is divided into two parts

$\Omega = \Omega^S + \Omega^L$, where Ω^S corresponds to collisions due to short range forces and Ω^L describes the effects of longer range interactions. It can be shown, starting from the BBGKY formalism and using a molecular chaos approximation, that long-range molecular interactions can be represented as a mean field[23] and thus incorporated into the body force term in Eq. (1). For example, in the limit of small density gradients, the mean field potential, due to long-range interactions for a single-component fluid is given by $V = -2a\rho - \kappa\nabla^2\rho$, where a and κ can be related to the molecular potential.[23] The local acceleration field to be used in Eq. (1) is $\mathbf{a} = \mathbf{F}/m$, where $\mathbf{F} = -\nabla V$. In addition, a hard sphere repulsion, based on the Enskog model may be easily included as described in Ref. 24. Figure 2 shows the phase diagram for a coexisting liquid/gas phases using the mean-field potential with hard-sphere repulsion. In this case, the modified BGK lattice Boltzmann method described earlier (first order approximation) was utilized. Similar calculations using the standard LB method was found to be unstable for $T/a < 0.71$ indicating the new approach is far more stable and allows for significantly larger density gradients or deeper quenches.

In conclusion, a framework for solution of the time evolution of the single-particle distribution function, which unifies standard kinetic theory with lattice Boltzmann methods was studied. In addition, the methods describe in this paper provide a clear link between Navier–Stokes based computational fluid dynamics approaches and lattice Boltzmann methods. Indeed, these approaches can be made

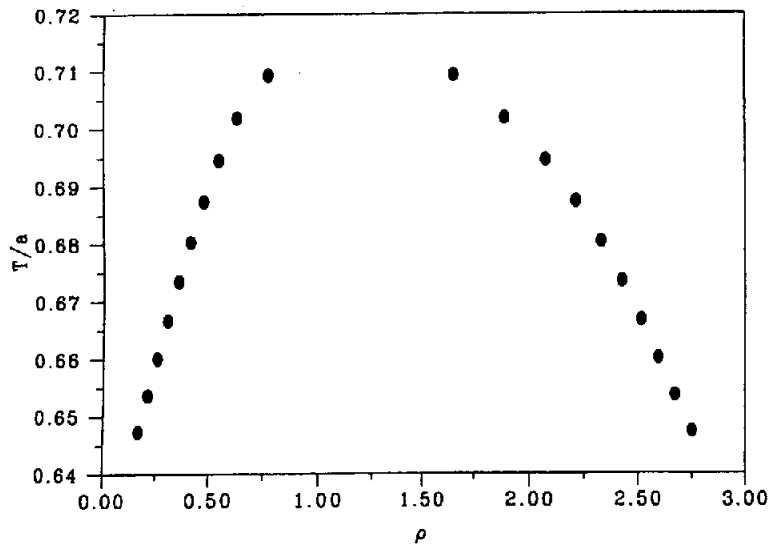

Fig. 2. Phase diagram for typical mean-field based model of fluid combining a long range attractive interaction with a hard sphere repulsion term. The fluid density is ρ and T/a is the ratio of temperature to interaction strength. Results were obtained using the LB model modified to only include terms up to first order as described in text. Standard LB methods could only model regions near the critical point, $T/a \approx 0.71$, as the algorithm become unstable for the systems studied.

interchangeable if desired. These methods should be of benefit for computational modeling of complex fluids in many areas of research.

Note Added in Review

It has been brought to my attention that an approach similar in spirit, to appoximate the Navier–Stokes equations, has been suggested by Junk and Rao,[25] which utilizes a Chapman–Enskog expansion of the single particle distribution function. In their approach, the single partice distribution function is free streamed as if it was in the post collision state of lattice Boltzmann. The difference between the approach of Junk and Rao and that described in this paper is that the BGK collision operator form (or, indeed, all of the Boltzmann–BGK equation) is preserved, to the order required, giving our approach a different physical interpretation. Also, the method of Junk and Rao, in the regime of large viscosity, will suffer from the same instabilities as described earlier. Again, this can be controlled by adapting a finite difference form of the LB BGK equation as suggested in this paper. Another minor point, in regards to computational memory, it was stated[25] that duplicates of ρ and $\mathbf{u}$ are needed to carry out calculations. We find that only a single copy is needed, hence reducing memory needs in half of that suggested by Junk and Rao.

References

1. I. Manas-Zloczower and Z. Tadmor, *Mixing and Compounding of Polymers: Theory and Practice, Progress in Polymer Processing Series* (Hanser-Publishers, Munich, 1994); J.-F. Agassant, P. Avenas, J.-Ph. Sergent, and P. J. Carreau, *Polymer Processing: Principles and Modeling* (Oxford University Press, New York, 1991).
2. M. A. Celia, H. Rajaram, and L. Ferrand, *Advances in Water Resources* **16**, 81 (1993).
3. P.-Z. Wong, *Physics Today* **41**, 24 (1998); F. A. L. Dullien, *Porous Media: Fluid Transport and Pore Structure* (Academic Press, San Diego, 1992); P. M. Adler, *Porous Media: Geometry and Transports* (Butterworth-Heinemann, Boston, 1992).
4. L. P. McMaster, *Adv. Chem. Ser.* **142**, 43 (1975); E. D. Siggia, *Phys. Rev. A* **20**, 595 (1970).
5. A. H. Krall, J. V. Sengers, and K. Hamano, *Phys. Rev. Lett.* **69**, 1963 (1992); E. K. Hobbie, L. Reed, C. C. Huang, and C. C. Han, *Phys. Rev. E* **48**, 1579 (1993); T. Hashimoto, K. Matsuzaka, E. Moses, and A. Onuku, *Phys. Rev. Lett.* **74**, 126 (1995).
6. J. F. Joanny and P. G. de Gennes, *J. Chem. Phys.* **81**, 552 (1984).
7. N. Martys, M. O. Robbins, and M. Cieplak, *Phys. Rev. B* **44**, 12294 (1991).
8. U. Frisch, B. Hasslacher, and Y. Pomeau, *Phys. Rev. Lett.* **56**, 1505 (1986).
9. D. H. Rothman and S. Zaleski, *Rev. Mod. Phys.* **66**, 1417 (1998).
10. R. Benzi, S. Succi, and M. Vergassola, *Phys. Rep.* **222**, 145 (1992).
11. H. Chen, S. Y. Chen, and W. H. Matthaeus, *Phys. Rev. A* **45**, R5339 (1992).
12. Y. H. Qian, D. d'Humières, and P. Lallemand, *Europhys. Lett.* **17**, 479 (1992).
13. X. Shan and H. Chen, *Phys. Rev. E* **47**, 1815 (1993).
14. M. R. Swift, W. R. Osborn, and J. M. Yeomans, *Phys. Rev. Lett.* **75**, 830 (1995).
15. N. S. Martys, X. Shan, and H. Chen, *Phys. Rev. E* **58**, 6855 (1998).
16. S. Chen, D. Martinez, and R. Mei, *Phys. Fluids* **8**, 2527 (1996).
17. R. L. Liboff, *Kinetic Theory*, 2nd edition (John Wiley & Sons, 1998).

18. S. Chapman and T. G. Cowling, *The Mathematical Theory of Non-Uniform Gases*, 3rd edition (Cambridge University Press, London, 1970).
19. M. L. de Haro, E. G. D. Cohen, and J. M. Kincaid, *J. Chem. Phys.*
20. Abe, *J. Comput. Phys.* **131**, 241 (1997); X. He and L. S. Luo, *Phys. Rev. E* **55**, R6663 (1997); X. Shan and X. He, *Phys. Rev. Lett.* **80**, 65 (1998).
21. N. S. Martys and J. F. Douglas, *Phys. Rev. E* **63**, 31205 (2001).
22. I. Ginzbourg and P. M. Adler, *J. Phys. II France* **4**, 191 (1994).
23. N. S. Martys, *Int. J. Mod. Phys. C* **10**, 1367 (1999).
24. X. He, X. Shan, and G. D. Doolen, *PRE* **50**, R13 (1998).
25. M. Junk and S. V. R. R. Rao, *JCP* **155**, 178 (1999).